

# **Shock Testing with Multi-Instrument – Classical Shock Pulses and Shock Response Spectrum**



Wang Hongwei  
(Ph.D)

Rev: 01  
Jan. 25, 2024

*Note: VIRTINS TECHNOLOGY reserves the right to make modifications to this document at any time without notice. This document may contain typographical errors.*

## TABLE OF CONTENTS

<b>1. INTRODUCTION .....</b>	<b>3</b>
<b>2. CLASSICAL SHOCK PULSES .....</b>	<b>3</b>
2.1 BASIC PULSE SHAPE .....	3
2.1.1 Half-Sine .....	3
2.1.2 Final-Peak Saw-Tooth .....	4
2.1.3 Trapezoidal .....	5
2.2 TESTING MACHINERY .....	6
2.3 MEASUREMENT HARDWARE .....	7
2.3.1 IEPE Accelerometer + IEPE Data Acquisition Hardware .....	7
2.3.2 Charge-Mode Accelerometer + Charge Data Acquisition Hardware .....	8
2.3.3 All-in-one Digital Accelerometers .....	9
2.4 MEASUREMENT SOFTWARE .....	9
2.4.1 Low Pass Filtering .....	9
2.4.2 Tolerance Limit Checking .....	10
2.4.2.1 Basic Pulse Shape .....	10
2.4.2.2 Velocity Change .....	12
2.4.2.3 Cross Axis Motion .....	14
<b>3. SHOCK RESPONSE SPECTRUM .....</b>	<b>14</b>
3.1 SHOCK RESPONSE SPECTRUM MODEL .....	16
3.1.1 Absolute Acceleration SRS .....	17
3.1.2 Relative Velocity SRS .....	17
3.1.3 Relative Displacement SRS .....	18
3.1.4 Pseudo Velocity SRS .....	18
3.1.5 Equivalent Static Acceleration SRS .....	18
3.2 SHOCK RESPONSE SPECTRUM CALCULATION .....	18
3.2.1 Ramp Invariant Method .....	18
3.2.2 Sampling Rate Considerations .....	19
3.3 SHOCK RESPONSE SPECTRUM EXAMPLES .....	20
3.3.1 Configuration of SRS in Multi-Instrument .....	20
3.3.2 Half-sine Pulse .....	21
3.3.2.1 Absolute Acceleration Shock Response Spectrum .....	21
3.3.2.2 Relative Velocity Shock Response Spectrum .....	22
3.3.2.3 Relative Displacement Shock Response Spectrum .....	23
3.3.2.4 Pseudo Velocity Shock Response Spectrum .....	24
3.3.2.5 Equivalent Static Acceleration Shock Response Spectrum .....	25
3.3.3 Car and Motorcycle Crash Test .....	26
3.3.3.1 Absolute Acceleration Shock Response Spectrum .....	27
3.3.3.2 Pseudo Velocity Shock Response Spectrum .....	27
3.3.3.3 Velocity Change .....	28
3.3.4 Barge Shock Test .....	29
3.3.4.1 Absolute Acceleration Shock Response Spectrum .....	30
3.3.4.2 Pseudo Velocity Shock Response Spectrum .....	30
3.3.5 Kobe Earthquake Signal .....	31
3.3.5.1 Absolute Acceleration Shock Response Spectrum .....	32
3.3.5.2 Pseudo Velocity Shock Response Spectrum .....	33

## 1. Introduction

Mechanical shock testing is a process used to evaluate how well a product (or structure) can withstand sudden mechanical impacts or shocks. This type of testing is particularly important for products that may experience rough handling, transportation, field operation or other conditions where they might be subjected to abrupt acceleration or deceleration. It serves as a means to identify design and manufacturing weaknesses, potential failures, and areas for improvement, and ensures that the product meets industry or regulatory standards for mechanical durability and reliability. It forms a critical part of product development and quality assurance in industries such as aerospace, automotive, electronics, and military applications.

A mechanical shock can be caused, for example, by impact, collision, drop, bump, earthquake, or explosion. The real-life transient acceleration time histories of these shocks could be recorded in-situ, but only some of them can be replicated using laboratory shock equipment. Traditionally, three “classical” shock pulses, half-sine pulse, final-peak sawtooth pulse, and trapezoidal pulse, with specified peak acceleration and duration, are employed to simulate the effect of the real-world shock pulses (e.g. transportation shock pulses). The shapes of these pulses are relatively simple to characterize in the time domain and convenient to produce in laboratories. They may or may not be replicas of the real shock environment. For real-world shock signals that are too complicated to be represented by a time domain mathematical function and impractical to reproduce in laboratories (e.g. pyroshocks), the challenge lies in creating a shock environment that is equivalent, in some sense, to the real-life scenario. This leads to the introduction of Shock Response Spectrum (SRS), a useful tool for characterizing arbitrary shock signals, estimating their damage potentials and specifying test levels. The SRS of a real-world shock signal can be uniquely derived from its waveform in the time domain. The result can then serve as the fundamental requirement for synthesizing a new waveform within the limitations of a laboratory environment.

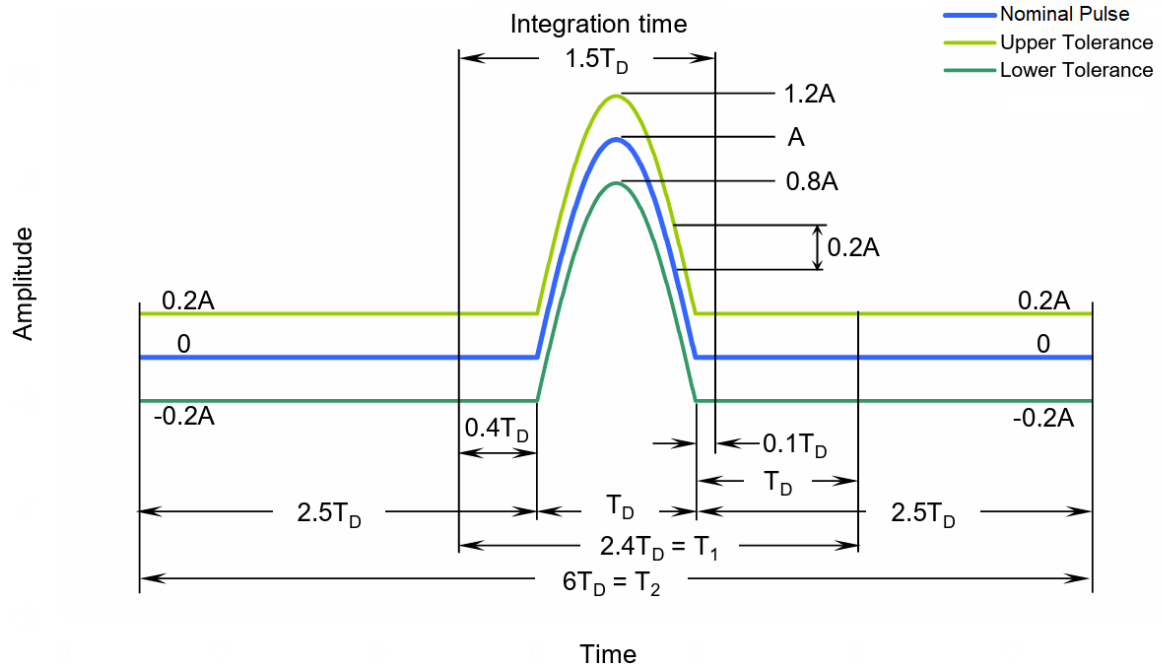
## 2. Classical Shock Pulses

### 2.1 Basic Pulse Shape

IEC 60068-2-27 defines three basic pulse shapes for classical shock testing.

#### 2.1.1 Half-Sine

A half-sine pulse comprises one half-cycle of a sine wave and is the most generally applicable. It has application when reproducing the effects of a shock resulting from impact with, or retardation by, a linear rate system, for example impact involving a resilient structure. The following figure shows a nominal half-sine pulse and its upper and lower limits of tolerance.



### Half-sine Pulse and Its Tolerance Limits

where:

$A$  = peak acceleration of nominal pulse

$T_D$  = duration of nominal pulse

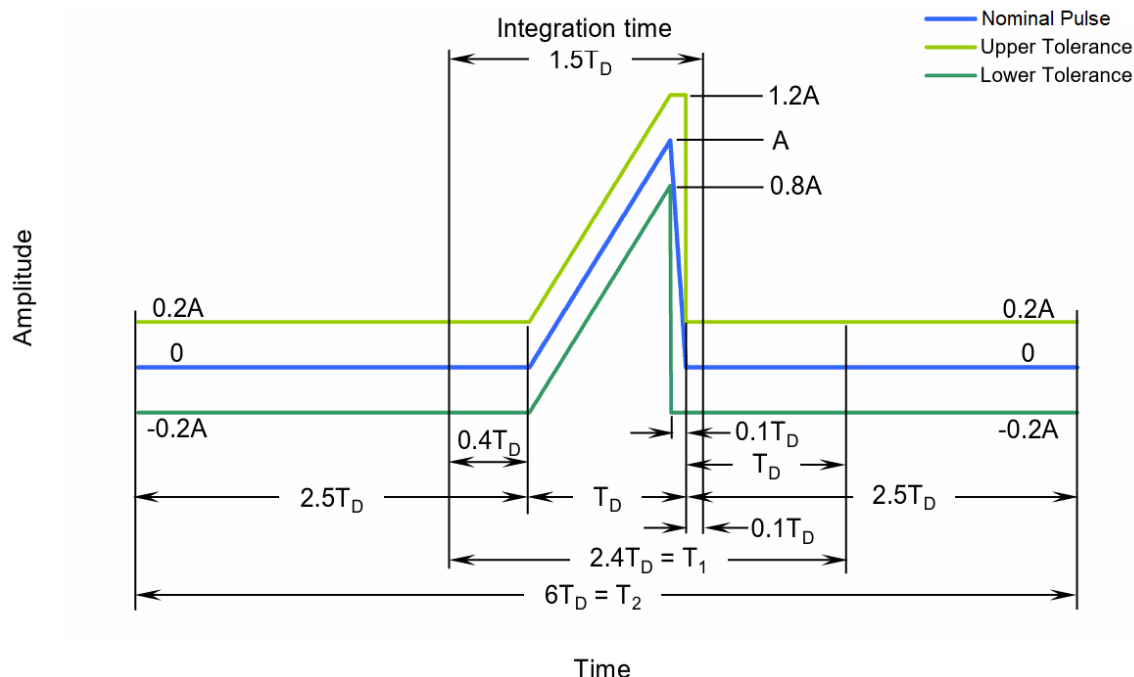
$T_1$  = minimum time during which the pulse shall be monitored for shocks produced using a conventional shock-testing machine

$T_2$  = minimum time during which the pulse shall be monitored for shocks produced using a vibration generator

Integration time: for derivation of velocity change from acceleration. The theoretical velocity change is given by:  $\frac{2}{\pi}AT_D$ . The actual velocity change shall be within  $\pm 15\%$  of it.

### 2.1.2 Final-Peak Saw-Tooth

A final-peak saw-tooth pulse consists of one cycle of an asymmetrical triangle wave with a short fall time, as shown the figure below. It has a more uniform response spectrum than the half-sine and trapezoidal pulse shapes.



### Final-peak Saw-tooth Pulse and Its Tolerance Limits

where:

A = peak acceleration of nominal pulse

$T_D$  = duration of nominal pulse

$T_1$  = minimum time during which the pulse shall be monitored for shocks produced using a conventional shock-testing machine

$T_2$  = minimum time during which the pulse shall be monitored for shocks produced using a vibration generator

Integration time: for derivation of velocity change from acceleration. The theoretical velocity change is given by:  $1/2AT_D$ . The actual velocity change shall be within  $\pm 15\%$  of it.

### 2.1.3 Trapezoidal

A trapezoidal pulse is made up of one cycle of a symmetrical trapezoid wave with short rise and fall times, as shown in the figure below. It produces a higher response over a wider frequency spectrum than the half-sine pulse. It should be applied when the purpose of the test is to reproduce the effects of shock environments such as the “explosive bolt” phase of a space probe / satellite launch.

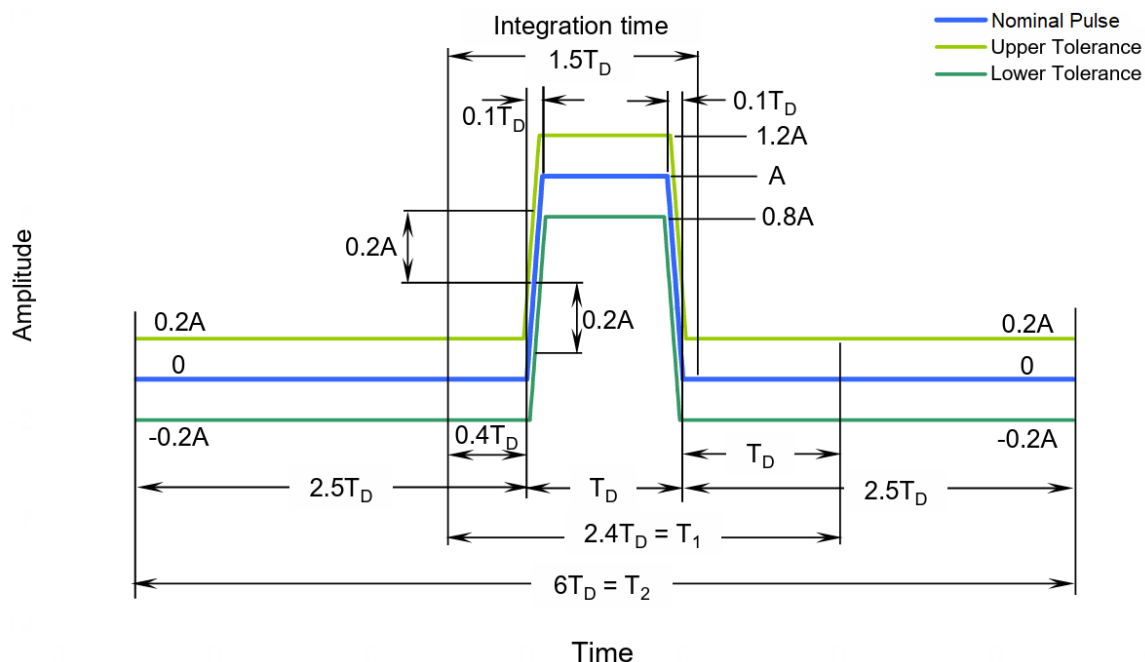
where:

A = peak acceleration of nominal pulse

$T_D$  = duration of nominal pulse

$T_1$  = minimum time during which the pulse shall be monitored for shocks produced using a conventional shock-testing machine

$T_2$  = minimum time during which the pulse shall be monitored for shocks produced using a vibration generator



### Trapezoidal Pulse and Its Tolerance Limits

where:

$A$  = peak acceleration of nominal pulse

$T_D$  = duration of nominal pulse

$T_1$  = minimum time during which the pulse shall be monitored for shocks produced using a conventional shock-testing machine

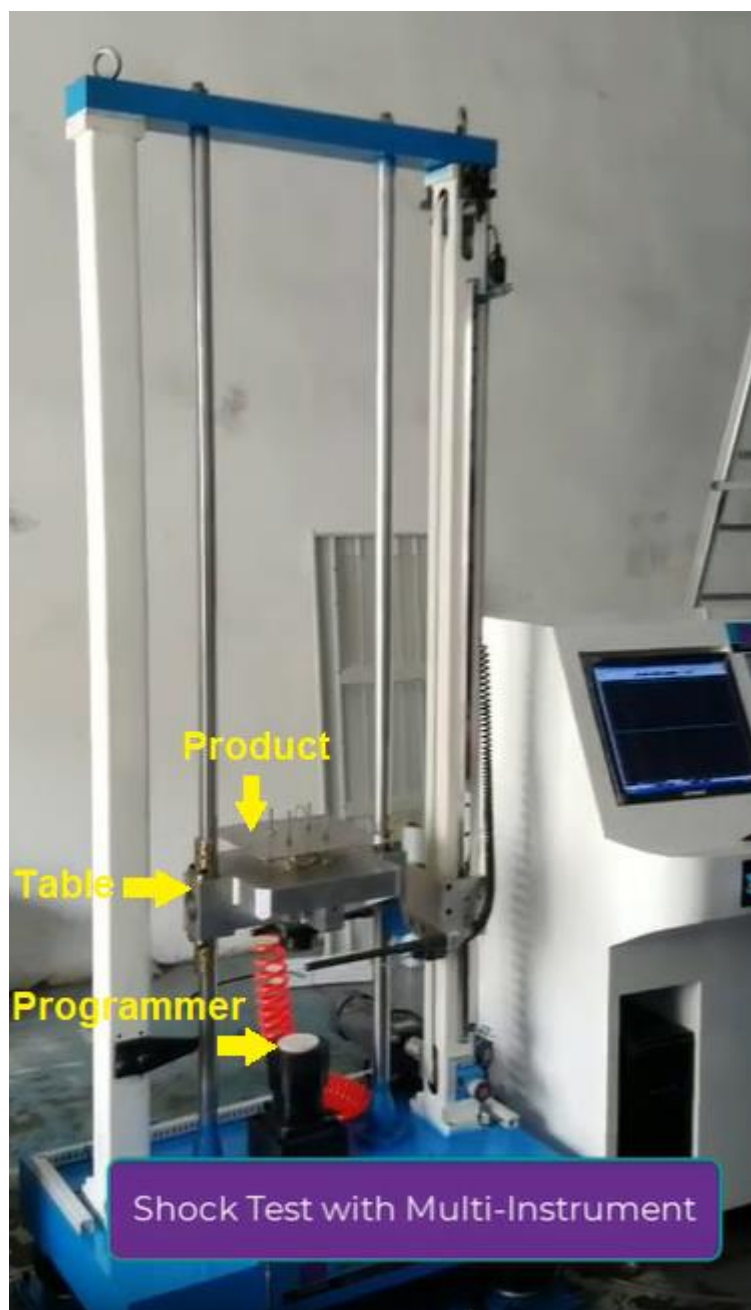
$T_2$  = minimum time during which the pulse shall be monitored for shocks produced using a vibration generator

Integration time: for derivation of velocity change from acceleration. The theoretical velocity change is given by:  $0.9AT_D$ . The actual velocity change shall be within  $\pm 15\%$  of it.

## 2.2 Testing Machinery

Classical shock testing can be performed on mechanical shock machines, electrodynamic shakers, or servo-hydraulic shakers. Mechanical shock machines do not have a closed-loop controller, unlike some of the shakers. Shakers are more controllable. They can generate more complicated shock and vibration signals. In order to run a classical shock test on a shaker, the pulse must start and end at zero acceleration, velocity, and displacement. Pre- and/or post-compensation pulses must be added to drive the shaker back to these zero parameters.

The most commonly used mechanical shock machine is the free-fall drop shock machine. One example is shown as follows. During a free-fall shock test, the product is mounted onto the table. The table is then raised to a height that corresponds to the target peak shock acceleration and dropped to the “ground”. The pulse shape and duration can be controlled using different programmers. Elastomer pads, such as rubber or felt, are typically employed for half-sine pulses. Deformable lead pellets are used for final-peak saw-tooth pulses, while aluminum honeycomb material or pneumatic cylinders are chosen for trapezoidal pulses.



**A Free-fall Drop Shock Machine**

## **2.3 Measurement Hardware**

The measurement hardware systems used in a shock test usually consist of piezoelectric accelerometers and data acquisition hardware. They can be classified into the following three categories.

### **2.3.1 IEPE Accelerometer + IEPE Data Acquisition Hardware**

IEPE stands for Integrated Electronics Piezo-Electric. IEPE sensors are equipped with built-in electronics to convert the high-impedance charge signal generated by a piezoelectric sensor into a low-impedance voltage signal that can be easily transmitted over a cable

without significant signal degradation. The sensor circuit is supplied with a constant current. A distinguishing feature of the IEPE principle is that the power supply and the sensor signal are transmitted via one shielded wire. Other proprietary names for IEPE are ICP, CCLD, IsoTron or DeltaTron.

A typical example of IEPE data acquisition hardware is VT IEPE-2G05 from Virtins Technology. Its BNC input connectors can be connected to IEPE sensors directly, and it works like a USB sound card with switchable input voltage ranges and digital filters.



**A typical example of IEPE Data Acquisition Systems**

### 2.3.2 Charge-Mode Accelerometer + Charge Data Acquisition Hardware

Unlike IEPE sensors, charge-mode sensors lack built-in electronics, allowing them to withstand higher temperatures and shocks more effectively. To minimize triboelectric noise, a specialized low-noise cable specifically designed for connecting the sensor to the input of a charge amplifier should be used.

A typical example of charge data acquisition hardware is VT CAMP-2G05 from Virtins Technology. Its BNC input connectors can be connected to charge-mode sensors directly, and it works like a USB sound card with switchable input charge ranges and digital filters.



**A typical example of Charge Data Acquisition Systems**



### 2.3.3 All-in-one Digital Accelerometers

USB digital accelerometers are all-in-one devices. Typical examples are Digiducer 333D01 and 333D04. They work like USB sound cards.



**A typical example of All-in-one Digital Accelerometers**

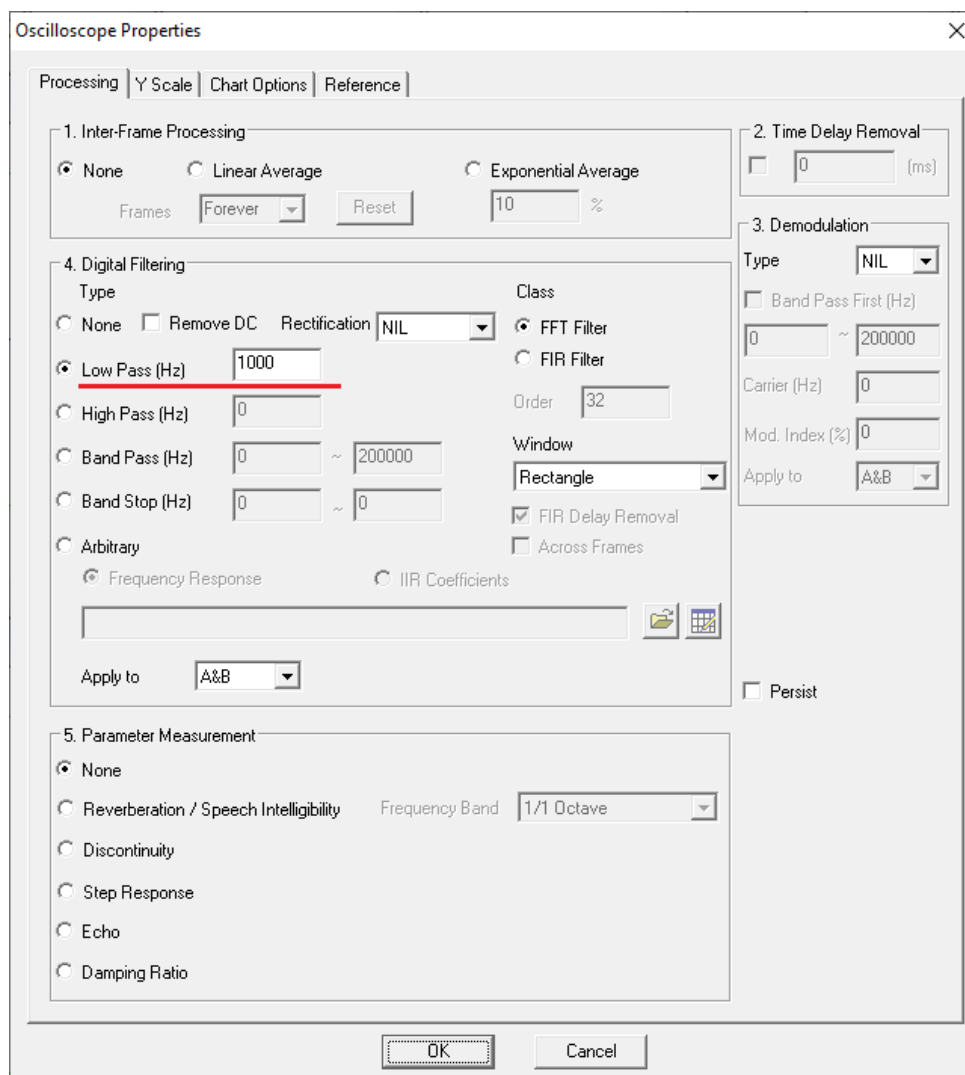
## 2.4 Measurement Software

A typical example of the measurement software is Multi-Instrument developed by Virtins Technology. It is a powerful multi-function virtual instrument software. It is a professional tool for time, frequency, time-frequency and modulation domain analyses. The software supports a variety of hardware ranging from sound cards which are available in almost all computers to proprietary ADC and DAC hardware such as NI DAQmx cards, VT DSO, VT RTA, VT IEPE, VT CAMP, RTX6001 and so on. It can be downloaded for 21-day fully functional free trial at: [www.virtins.com](http://www.virtins.com).

### 2.4.1 Low Pass Filtering

The acceleration waveform measured in a shock test usually exhibits high-frequency fluctuations along the nominal shape. Low pass filtering is commonly employed to smooth the waveform before conducting tolerance limit checking. The -3dB cutoff frequency of the low pass filter should not be lower than  $1.5/T_D$  and its phase response should be kept as linear as possible to ensure that the induced deformation from the basic pulse shape remains negligible.

Multi-Instrument supports three classes of digital filtering: FFT, FIR, and IIR. FFT is generally recommended here due to its zero phase response. The following shows the configuration of a low pass FFT filter.



**Configuration of Digital Filtering in Multi-Instrument**

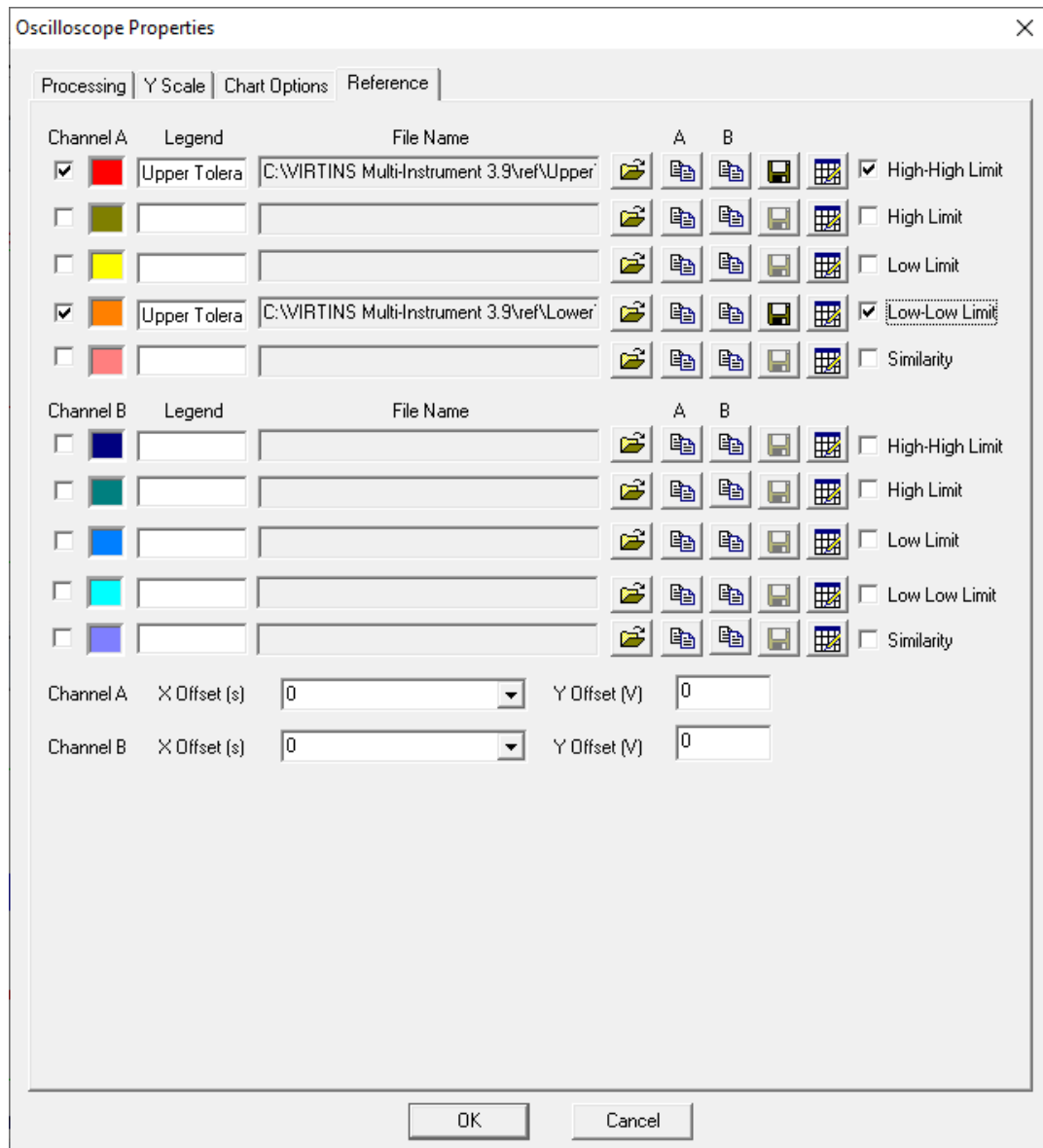
## 2.4.2 Tolerance Limit Checking

Shock severity is the combination of the peak acceleration, the duration of the nominal pulse and the number of shocks. Wherever possible, the test severity and the shape of the shock pulse applied to the specimen should be such as to reproduce the effects of the actual transport or operational environment to which the specimen will be subjected, or to satisfy the design requirements if the object of the test is to assess structural integrity. Tolerance limit checking on basic pulse shape, velocity change, and cross axis motion shall be performed to ensure a high degree of reproducibility of the shock testing.

### 2.4.2.1 Basic Pulse Shape

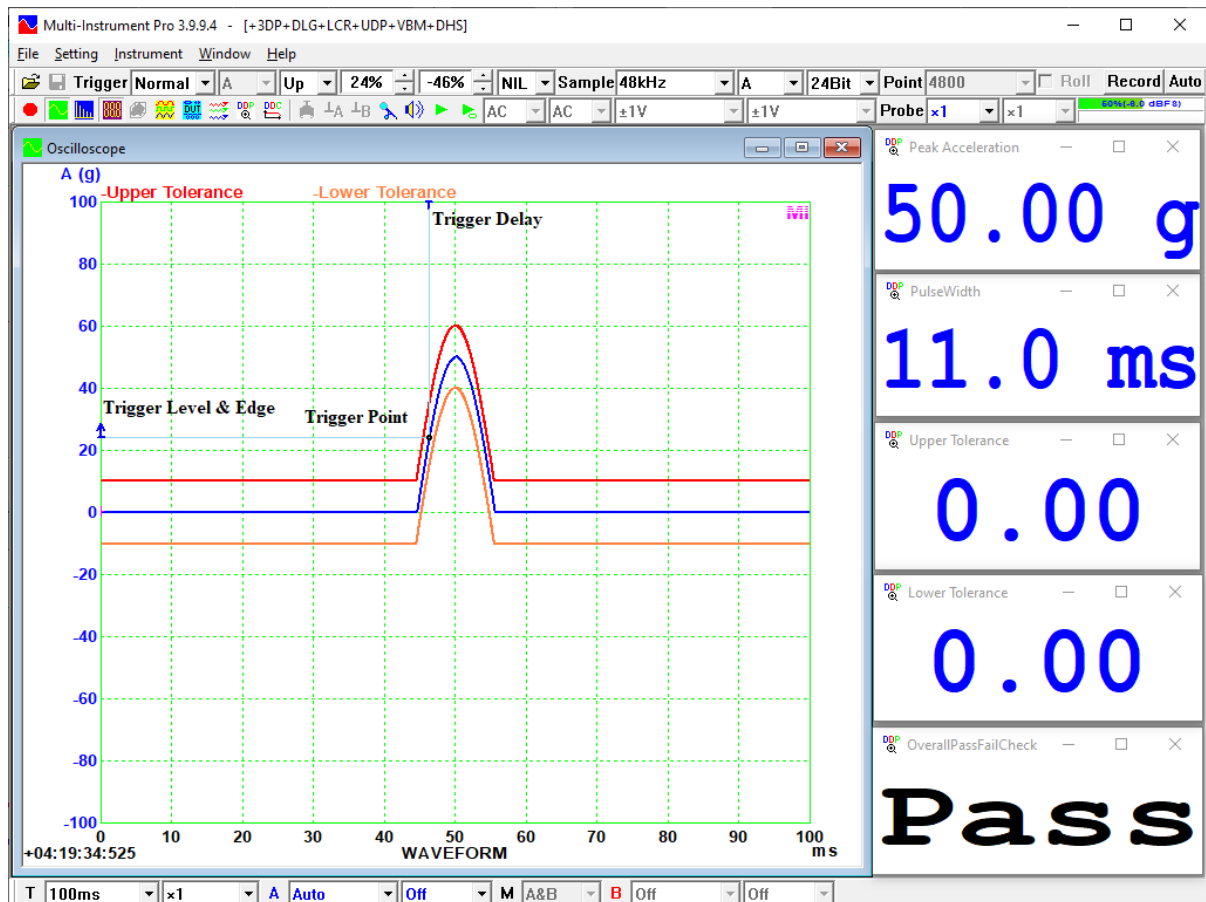
In Multi-Instrument, Trigger Mode, Trigger Source, Trigger Edge, Trigger Level, Trigger Delay, and Trigger Frequency Rejection can be adjusted so as to capture the shock waveform at the right position (e.g. center) along the X axis of the Oscilloscope window. The tolerance limits of the basic pulse shape can be defined by CSV text files and then configured as Reference curves, as shown as follows. The reference curves can be aligned to the captured

waveform along the X axis automatically if either “Align to Peak” or “Align to Trough” is selected for the X Offset (s), otherwise the manually entered offset value will be used.



**Reference Curve (Tolerance Limit) Configuration in Multi-Instrument**

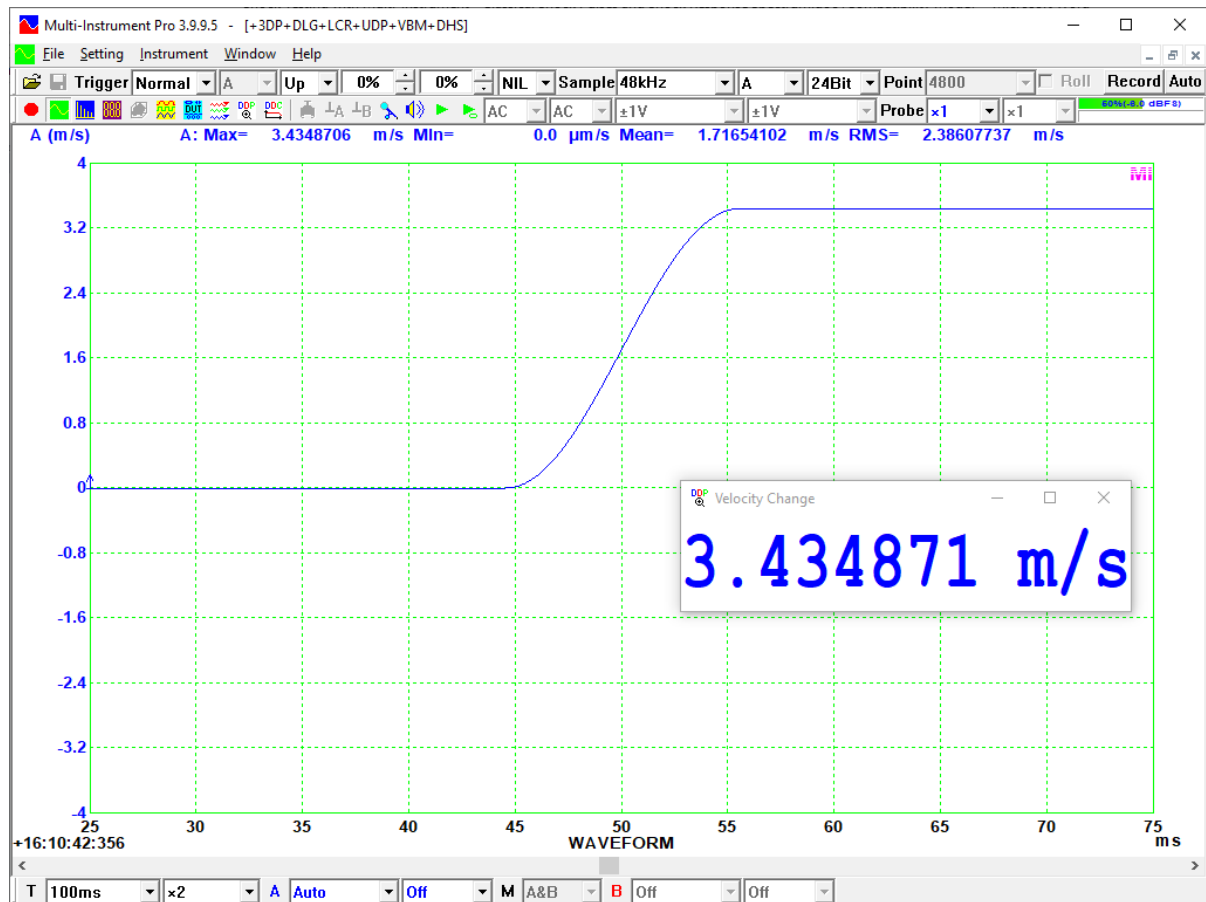
The following screenshot shows an example of waveform positioning and tolerance limit checking using Multi-Instrument.



**Positioning of Waveform and Tolerance Limit Checking in Multi-Instrument**

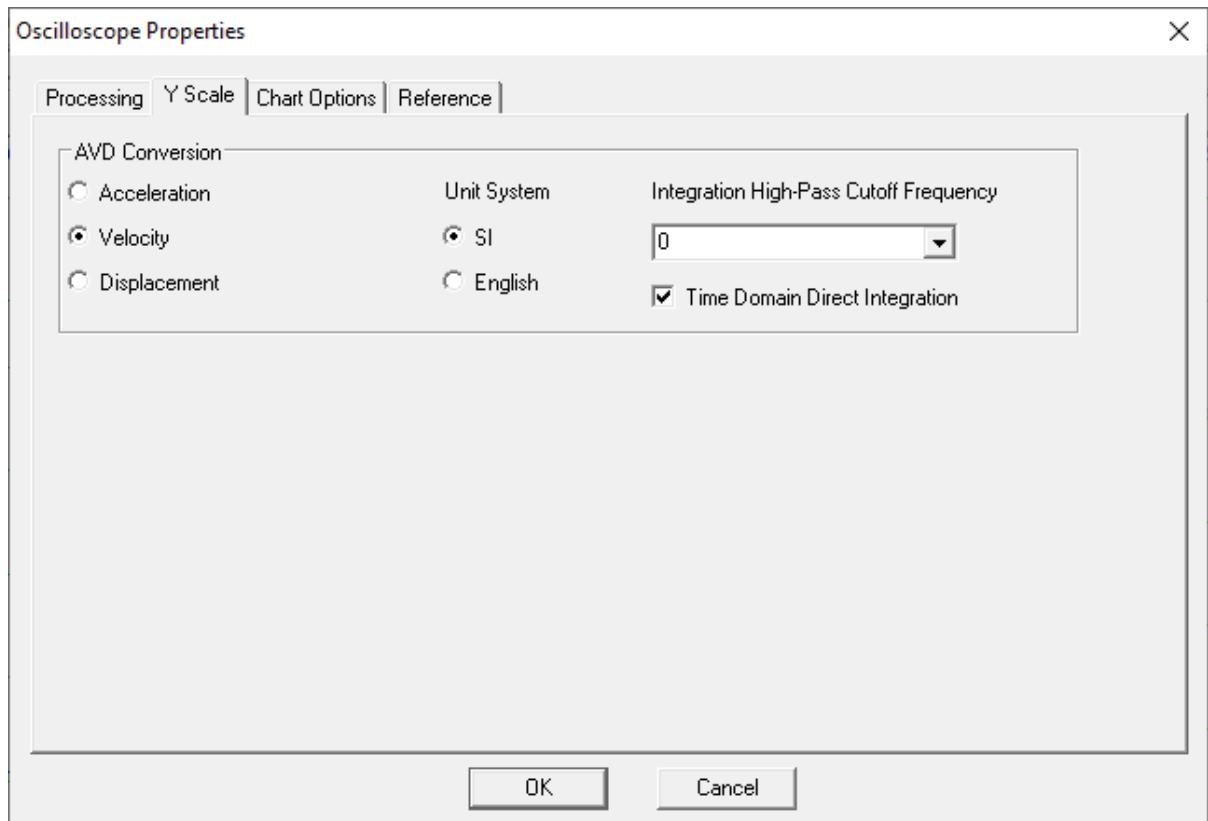
#### 2.4.2.2 Velocity Change

As mentioned previously, the actual velocity change shall be within  $\pm 15\%$  of the theoretical value corresponding to the nominal pulse. The following screenshot shows the velocity (change) variation with time during a 11ms 50g half-sine shock pulse (i.e. the shock pulse shown previously).



**Velocity Variation Obtained by Time-domain Direct Integration in Multi-Instrument**

Conversion from acceleration to velocity and subsequently to displacement requires integration and double integration respectively. Multi-Instrument supports integration in either the time domain or the frequency domain. The velocity change measured in the screenshot above was obtained through time domain direct integration in Multi-Instrument (see configuration below).



**Acceleration, Velocity & Displacement Conversion Configuration in Multi-Instrument**

2.4.2.3 Cross Axis Motion

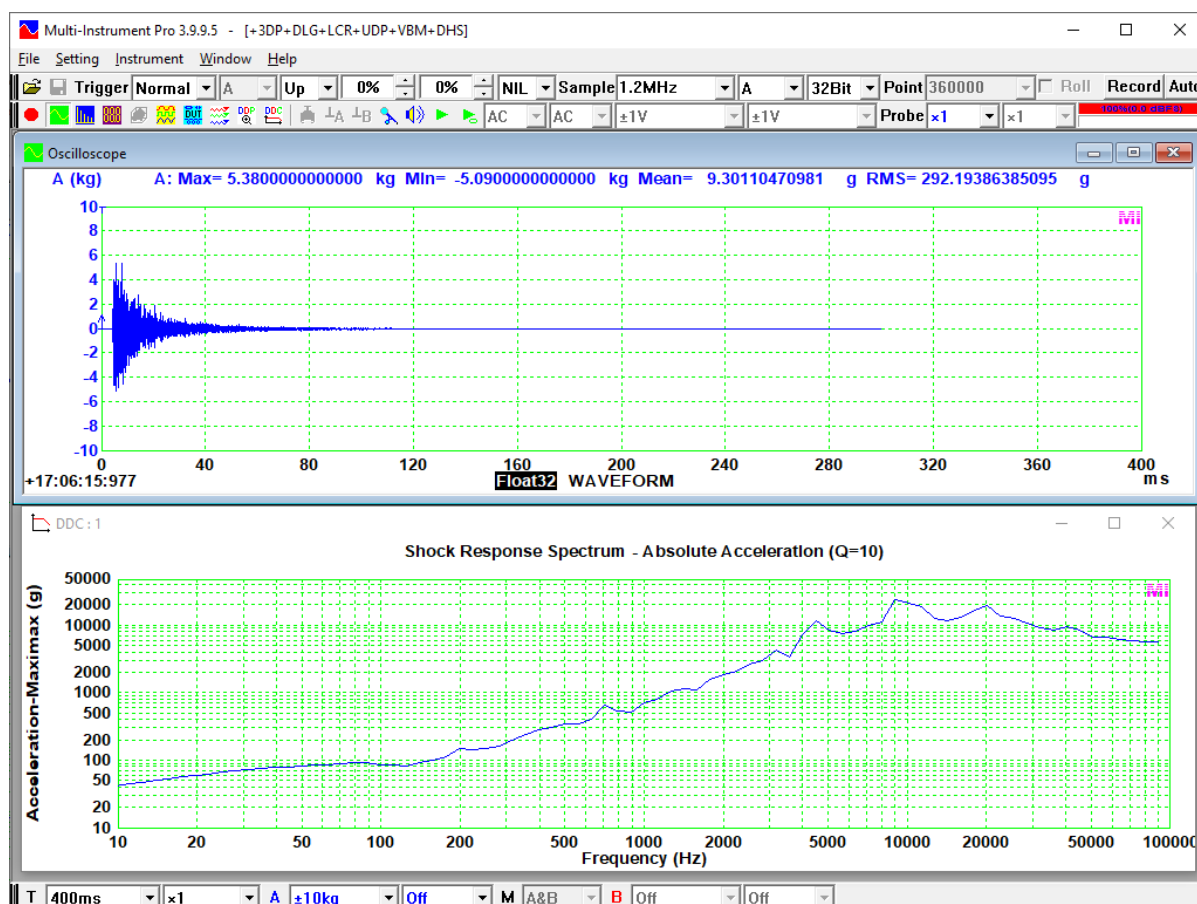
The cross axis motion, perpendicular to the intended shock direction, shall not exceed 30% of the value of the peak acceleration of the nominal pulse in the intended direction.

**3. Shock Response Spectrum**



**Rocket Hot-stage Separation**

Shock Response Spectrum (SRS) is a graphical representation of an arbitrary transient acceleration input, such as a shock, in terms of how a Single Degree Of Freedom (SDOF) system (like a mass on a spring) would respond to that input. The horizontal axis shows the natural frequency of a hypothetical SDOF system, and the vertical axis shows the peak acceleration, velocity or displacement, which this SDOF system would undergo as a consequence of the shock input. The following screenshot shows a typical pyrotechnic pulse and the corresponding absolute acceleration SRS (Quality factor  $Q=10$ , or Damping Ratio  $\xi=0.05$ ).

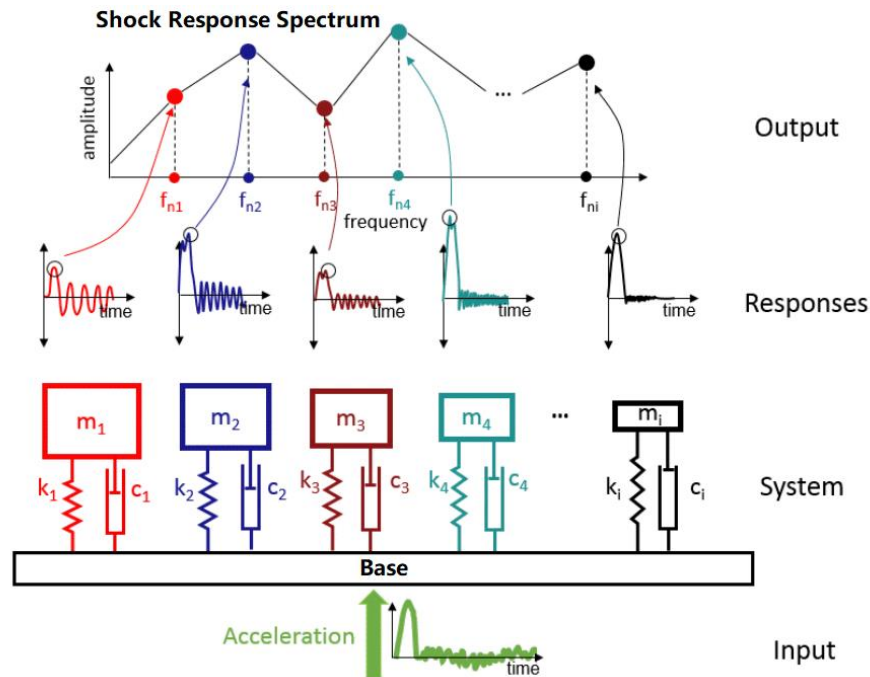


### A Pyrotechnic Pulse and Its Absolute Acceleration SRS

The pyrotechnic pulse above has a complex waveform. It tends to oscillate in a somewhat symmetric manner about the zero baseline. Its overall envelope has an exponential decay. Reproducing the pyrotechnic pulse for a product qualification test using mechanical equipment in laboratories would be virtually impossible. To address this challenge, the common industry practice is to use the SRS (not the waveform) of the pyrotechnic pulse as the specification instead to synthesize a waveform with a likely similar damage potential. This process is called Shock Response Synthesis. There are an infinite number of waveforms that have the same SRS. Shock Response Synthesis will need to find a solution that fits within the limits of the laboratory equipment.

### 3.1 Shock Response Spectrum Model

Given the time history of a transient acceleration input, a series of SDOF (Single Degree Of Freedom) systems with different natural frequencies and the same damping ratio can be used to calculate its SRS, as illustrated in the following figure.



**Shock Response Spectrum Model**

The given acceleration input  $a_1$  is applied to the common base of the group of independent SDOF systems. Each SDOF system has a unique set of mass  $m$ , damping constant  $c$ , and spring constant  $k$ . Its undamped Natural Frequency  $f_n$ , Resonance Gain (or Quality Factor)  $Q$ , and Damping Ratio  $\zeta$ , are given by the following three equations:

$$f_n = \frac{1}{2\pi} \sqrt{\frac{k}{m}}$$

$$Q = \frac{\sqrt{km}}{c}$$

$$\zeta = \frac{1}{2Q} = \frac{c}{2\sqrt{km}}$$

The SRS was composed of the maximum responses of each SDOF systems against their respective natural frequencies. Generally, there are five types of responses that interest various industries: Absolute Acceleration, Relative Velocity, Relative Displacement, Pseudo Velocity, and Equivalent Static Acceleration. For instance, Absolute Acceleration SRS is frequently employed in product qualification tests in aerospace and defense engineering, while Relative Velocity SRS is of greater interest in naval shock testing. The responses of a



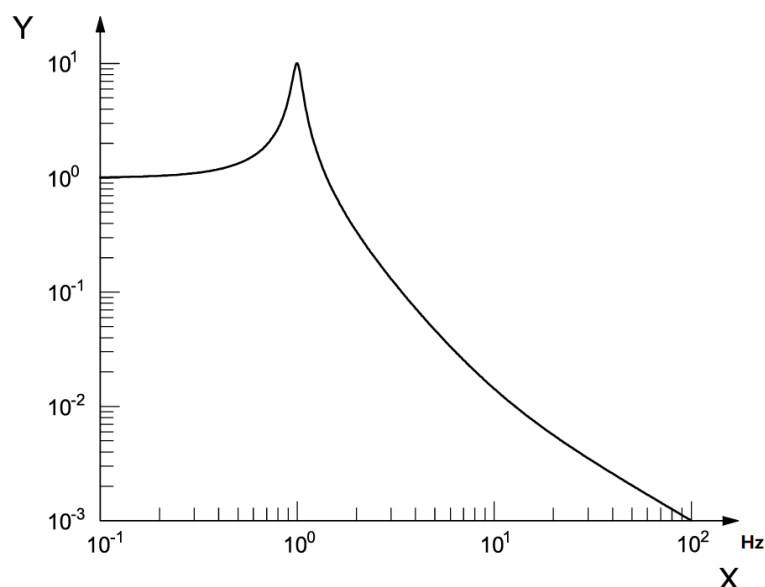
SDOF system to the acceleration input can be derived from the corresponding transfer functions.

### 3.1.1 Absolute Acceleration SRS

For a SDOF system, the transfer function  $G(s)$  between the base acceleration input  $a_1$  and the acceleration response  $a_2$  is given by:

$$G(s) = \frac{a_2(s)}{a_1(s)} = \frac{cs + k}{ms^2 + cs + k} = \frac{\frac{\omega_n s}{Q} + \omega_n^2}{s^2 + \frac{\omega_n s}{Q} + \omega_n^2}$$

where  $s$  is the Laplace variable (complex frequency) in radians per second, and  $\omega_n = 2\pi f_n$ , the angular natural frequency in radians per second. The following figure shows the transfer function of a SDOF system with a natural frequency of 1Hz (i.e.  $f_n = 1\text{Hz}$ ) and resonance gain of 10 (i.e.  $Q = 10$ ), as an example. Note that the transfer function is a function of the excitation signal frequency rather than the natural frequency, unlike SRS.



**Acceleration-to-Acceleration Transfer Function of a SDOF System**

### 3.1.2 Relative Velocity SRS

For a SDOF system, the transfer function  $G(s)$  between the base acceleration input  $a_1$  and the relative velocity response  $V_2 - V_1$  is given by:

$$G(s) = \frac{v_2(s) - v_1(s)}{a_1(s)} = \frac{-ms}{ms^2 + cs + k} = \frac{-s}{s^2 + \frac{\omega_n s}{Q} + \omega_n^2}$$

### 3.1.3 Relative Displacement SRS

For a SDOF system, the transfer function  $G(s)$  between the base acceleration input  $a_1$  and the relative displacement response  $d_2-d_1$  is given by:

$$G(s) = \frac{d_2(s) - d_1(s)}{a_1(s)} = \frac{-m}{ms^2 + cs + k} = \frac{-1}{s^2 + \frac{\omega_n s}{Q} + \omega_n^2}$$

### 3.1.4 Pseudo Velocity SRS

Pseudo velocity response can be calculated by multiplying the relative displacement response with the angular natural frequency  $\omega_n$ . Thus, the transfer function becomes:

$$G(s) = \frac{d_2(s) - d_1(s)}{a_1(s)} \cdot \omega_n = \frac{-m\omega_n}{ms^2 + cs + k} = \frac{-\omega_n}{s^2 + \frac{\omega_n s}{Q} + \omega_n^2}$$

### 3.1.5 Equivalent Static Acceleration SRS

Equivalent static acceleration response can be calculated by multiplying the relative displacement response with the squared angular natural frequency  $\omega_n^2$ . Thus, the transfer function becomes:

$$G(s) = \frac{d_2(s) - d_1(s)}{a_1(s)} \cdot \omega_n^2 = \frac{-m\omega_n^2}{ms^2 + cs + k} = \frac{-\omega_n^2}{s^2 + \frac{\omega_n s}{Q} + \omega_n^2}$$

## 3.2 Shock Response Spectrum Calculation

### 3.2.1 Ramp Invariant Method

The five types of responses of a SDOF system can be calculated by feeding the digitized input acceleration signal to a set of digital filters that approximate the aforementioned transfer functions. Several methods exist to design a digital filter based on a given analog transfer function, with the Ramp Invariant Algorithm being the most widely used, as defined in ISO 18431-4. In this algorithm, the digital filters corresponding to the five types of responses are second-order Infinite Impulse Response (IIR) filters with the following general z-transform expression:

$$H(z) = \frac{\beta_0 + \beta_1 \cdot z^{-1} + \beta_2 \cdot z^{-2}}{1 + \alpha_1 \cdot z^{-1} + \alpha_2 \cdot z^{-2}}$$

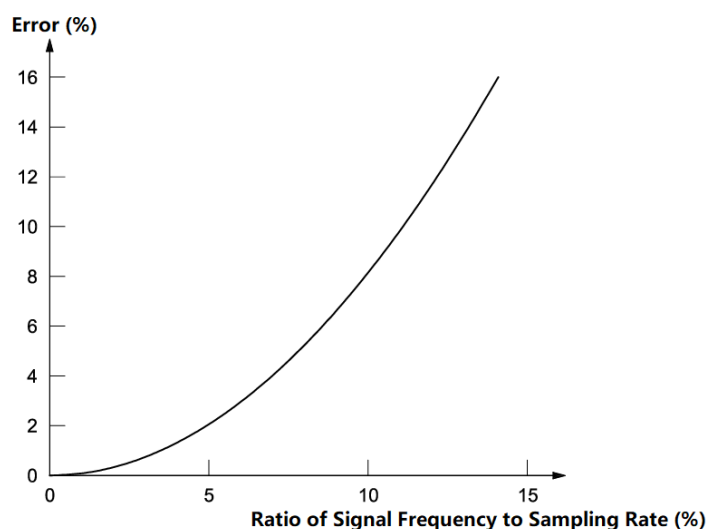
or in the time domain:

$$y_n = \beta_0 \cdot x_n + \beta_1 \cdot x_{n-1} + \beta_2 \cdot x_{n-2} - \alpha_1 \cdot y_{n-1} - \alpha_2 \cdot y_{n-2}$$

where  $x_n$  is the input acceleration time series,  $y_n$  the response time series,  $\beta_n$  feedforward filter coefficients, and  $\alpha_n$  feedback filter coefficients. The filter coefficients are determined by the type of response, the sampling rate  $f_s$ , the natural frequency  $f_n$  and resonance gain  $Q$  of the SDOF system.

### 3.2.2 Sampling Rate Considerations

The Ramp Invariant Algorithm contains a bias error that increases as the ratio of the signal frequency to the sampling rate grows. Another source of error arises from the fact that the peak in the sampled response signal is only an estimation of the “true” peak, which can fall between samples. The combination of these two errors results in a total maximum error of about 2% at 5% of the sampling rate, and 8% at 10% of the sampling rate, as shown in the following figure.



#### Total Maximum Error in Shock-Response Spectrum Calculation

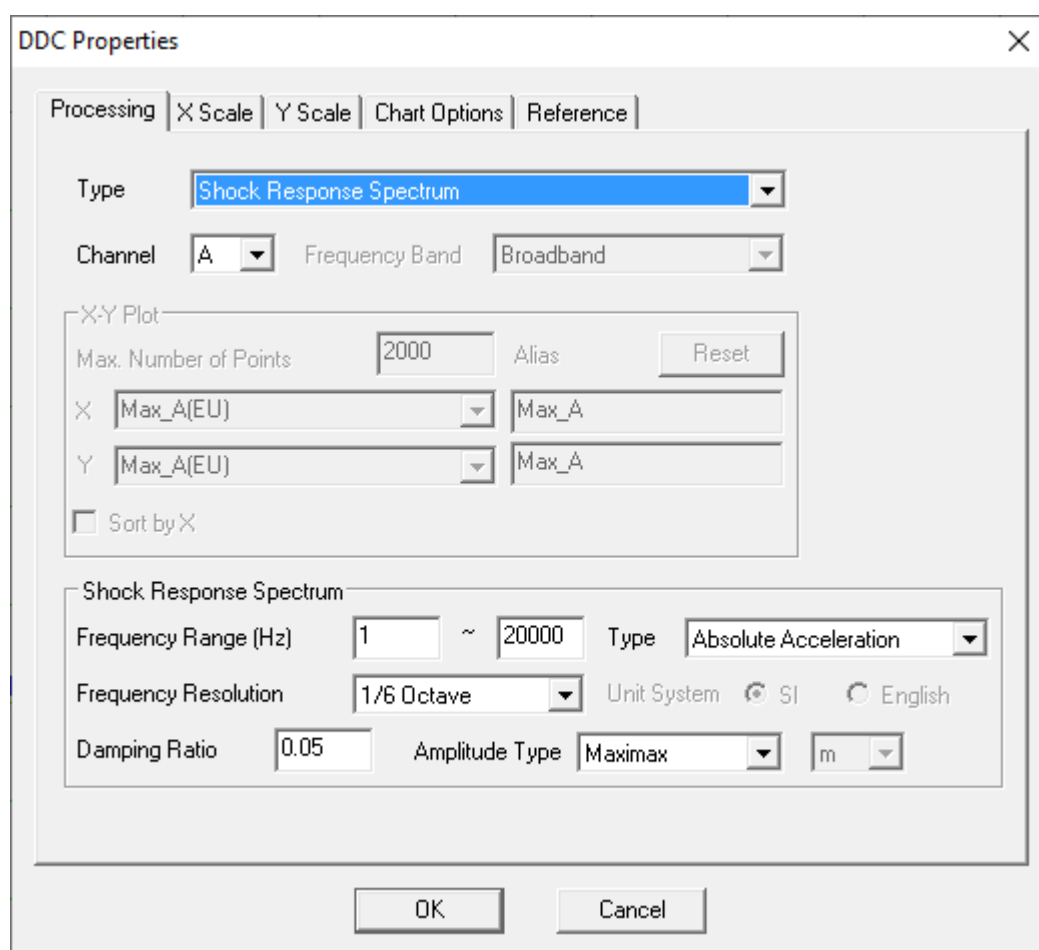
Therefore, the sampling rate should be at least 10 times the highest significant frequency content of the input signal. Multi-Instrument features a special algorithm that can up-sample the input signal and then calculate the SRS at a  $\times 32$  sampling rate internally. Thus, the calculated SRS will maintain its high accuracy even at the Nyquist frequency, which is half of the sampling rate. This algorithm works exceptionally well, especially for those data acquisition hardware devices that have a brick-wall anti-aliasing filter, such as VT IEPE-2G05 series and VT CAMP-2G05 series.

### 3.3 Shock Response Spectrum Examples

The acceleration data used in the following examples can be downloaded from: <https://www.virtins.com/doc/ShockResponseSpectrumAccelerationData.zip>. They are in CSV TXT format, and can be imported into Multi-Instrument via [File]>[Import].

#### 3.3.1 Configuration of SRS in Multi-Instrument

Multi-Instrument supports SRS through Derived Data Curves (DDC). The following figure shows the SRS configuration.



#### Configuration of SRS in Multi-Instrument

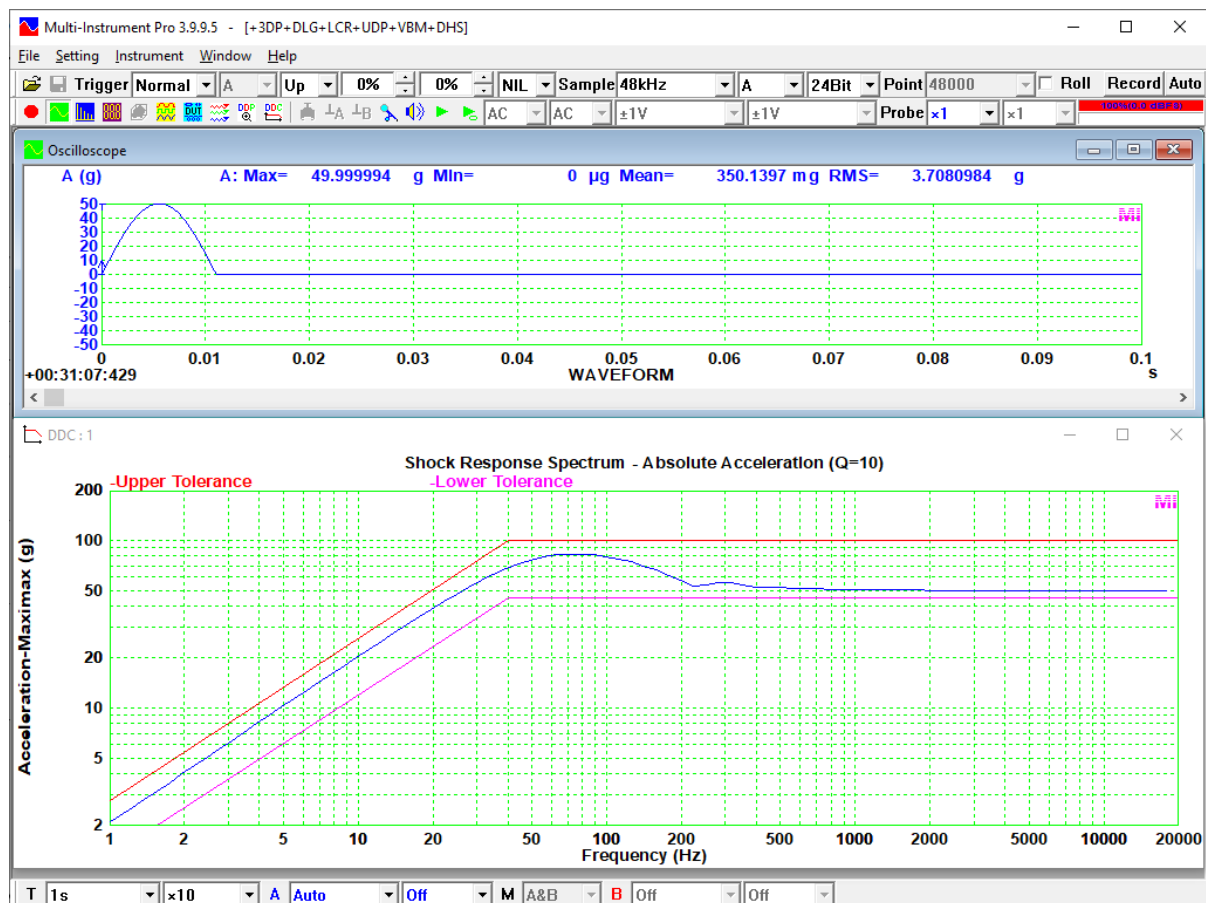
Five types of SRS can be calculated based on Ramp Invariant Algorithm: Absolute Acceleration, Relative Velocity, Relative Displacement, Pseudo Velocity, and Equivalent Static Acceleration. They can be represented in either SI or English units. For SI units, options for velocity and displacement scaling include 'm' (meters), 'dm' (decimeters), 'cm' (centimeters), and 'mm' (millimeters). The natural frequencies used for SRS calculation are chosen with the specified octave or fractional octave spacing within the specified frequency range. The damping ratio is configurable, typically 5% (i.e.  $Q=10$ ) should be used. Three response amplitude types are supported: Maximax (Maximum Absolute), Max+ (Maximum Positive) and Max- (Maximum Negative). The time record of the transient acceleration input should be long enough to be able to accommodate the important part (which contains the

Maximum Positive and Maximum Negative) of the response of any of the SDOF systems used in the calculation. Usually, 1/6 octave spacing is used for the natural frequencies when the damping ratio is in the range of 0.02~0.1, while 1/12 and 1/3 octave spacings are used when the damping ratio is below and beyond that range respectively.

### 3.3.2 Half-sine Pulse

#### 3.3.2.1 Absolute Acceleration Shock Response Spectrum

The following figures show the absolute acceleration SRS of a half-sine pulse, with a duration of 11 ms and a peak acceleration of 50g. The damping ratio used is 5% (i.e.  $Q=10$ ). The tolerance limits are also displayed.



**Absolute Acceleration SRS of a Half-sine Pulse**

It can be seen from the figure above that the SRS can be divided into three sections based on the natural frequency:

(1) *Natural Frequency*  $f_n < 26\text{Hz}$

The peak acceleration response is lower than the peak acceleration input (50g), meaning that the input is attenuated or “isolated”. The initial slope of the SRS is about 6dB/octave, that is, the peak acceleration response doubles when the natural frequency doubles. It represents a constant velocity line.

(2)  $26\text{Hz} \leq \text{Natural Frequency } f_n \leq 225\text{Hz}$

The peak acceleration response is higher than the peak acceleration input (50g), meaning that the input is amplified by the SDOF systems. The SRS is peaked at about 75Hz with a peak value of about 83g.

(3) *Natural Frequency*  $f_n > 225\text{Hz}$

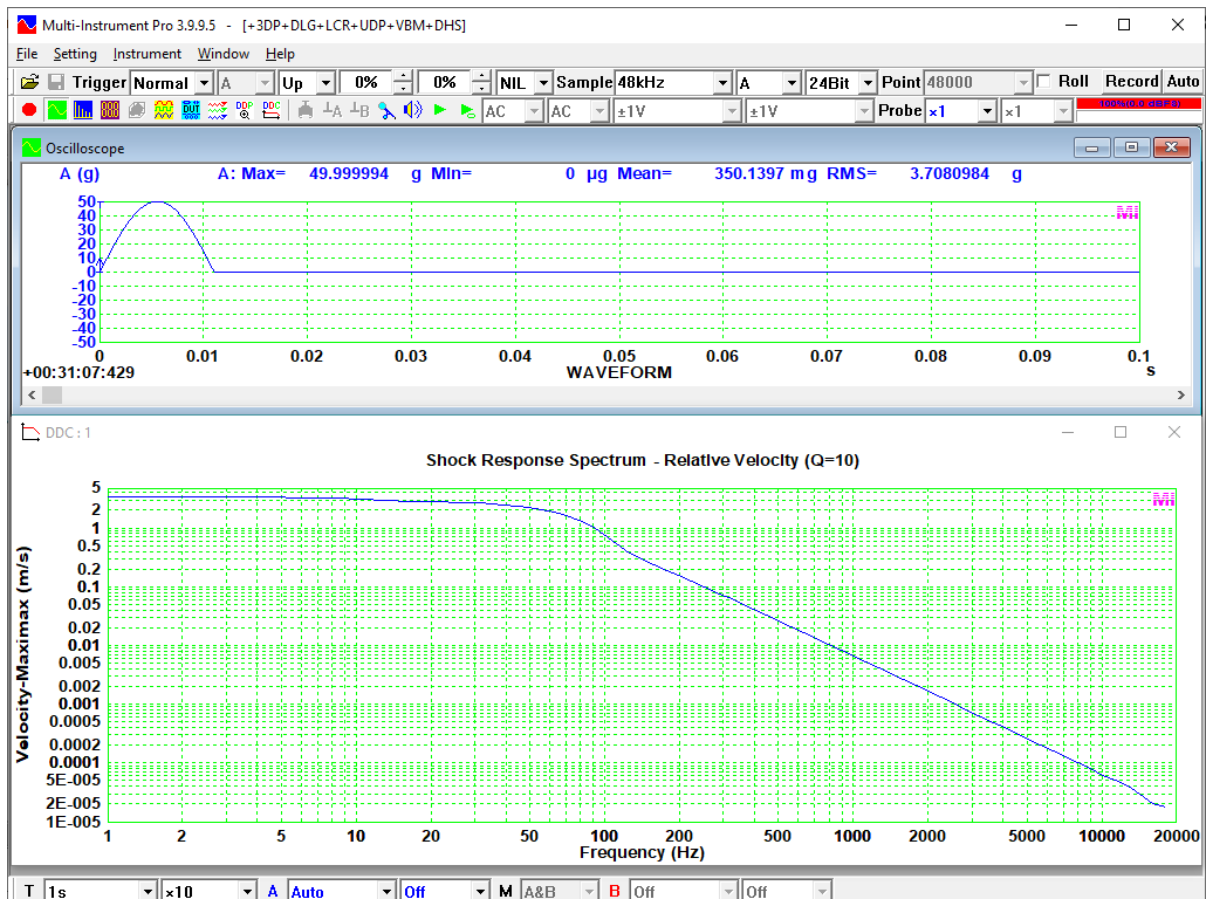
The peak acceleration response is more or less the same as the peak acceleration input (50g), meaning that the SDOF systems are “hard mounted” and track the input.

The table below summarizes the demarcation of the above three sections on SRS in a more general manner for the three classical shock pulses.

	Attenuated	Amplified	Hard Mounted
Half-sine	$f_n < 0.3/T_D$	$0.3/T_D \leq f_n \leq 3/T_D$ (Peak amplification of 1.7 at $0.8/T_D$ )	$f_n > 3/T_D$
Final-Peak Saw-tooth	$f_n < 0.4/T_D$	$0.4/T_D \leq f_n \leq 1.2/T_D$ (Peak amplification of 1.3 at $0.65/T_D$ )	$f_n > 1.2/T_D$
Trapezoidal	$f_n < 0.2/T_D$	$0.2/T_D \leq f_n \leq 10/T_D$ (Peak amplification of 2.0 at $0.55/T_D$ )	$f_n > 10/T_D$

### 3.3.2.2 Relative Velocity Shock Response Spectrum

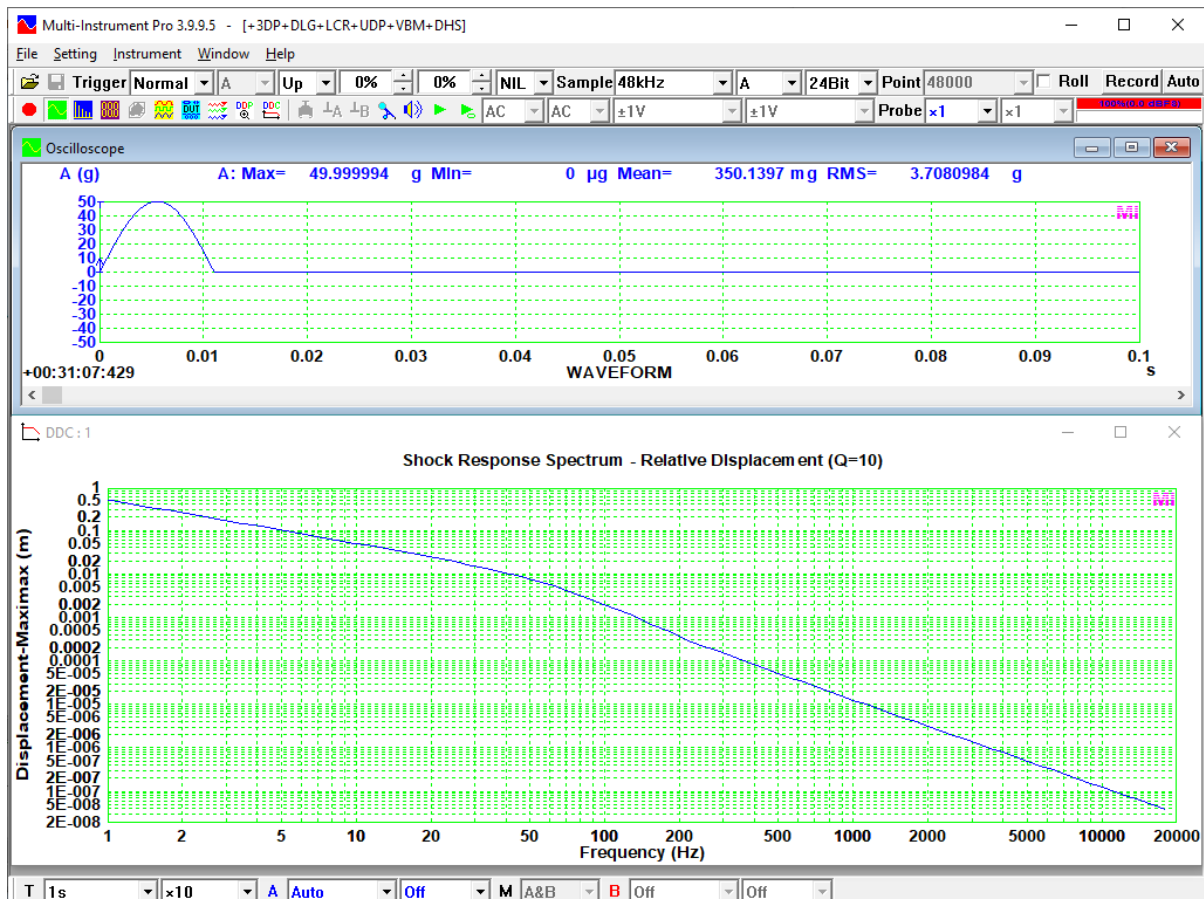
The following figures show the relative velocity SRS of a half-sine pulse, with a duration of 11 ms and a peak acceleration of 50g. The damping ratio used is 5% (i.e.  $Q=10$ ).



**Relative Velocity SRS of a Half-sine Pulse**

### 3.3.2.3 Relative Displacement Shock Response Spectrum

The following figures show the relative displacement SRS of a half-sine pulse, with a duration of 11 ms and a peak acceleration of 50g. The damping ratio used is 5% (i.e. Q=10).

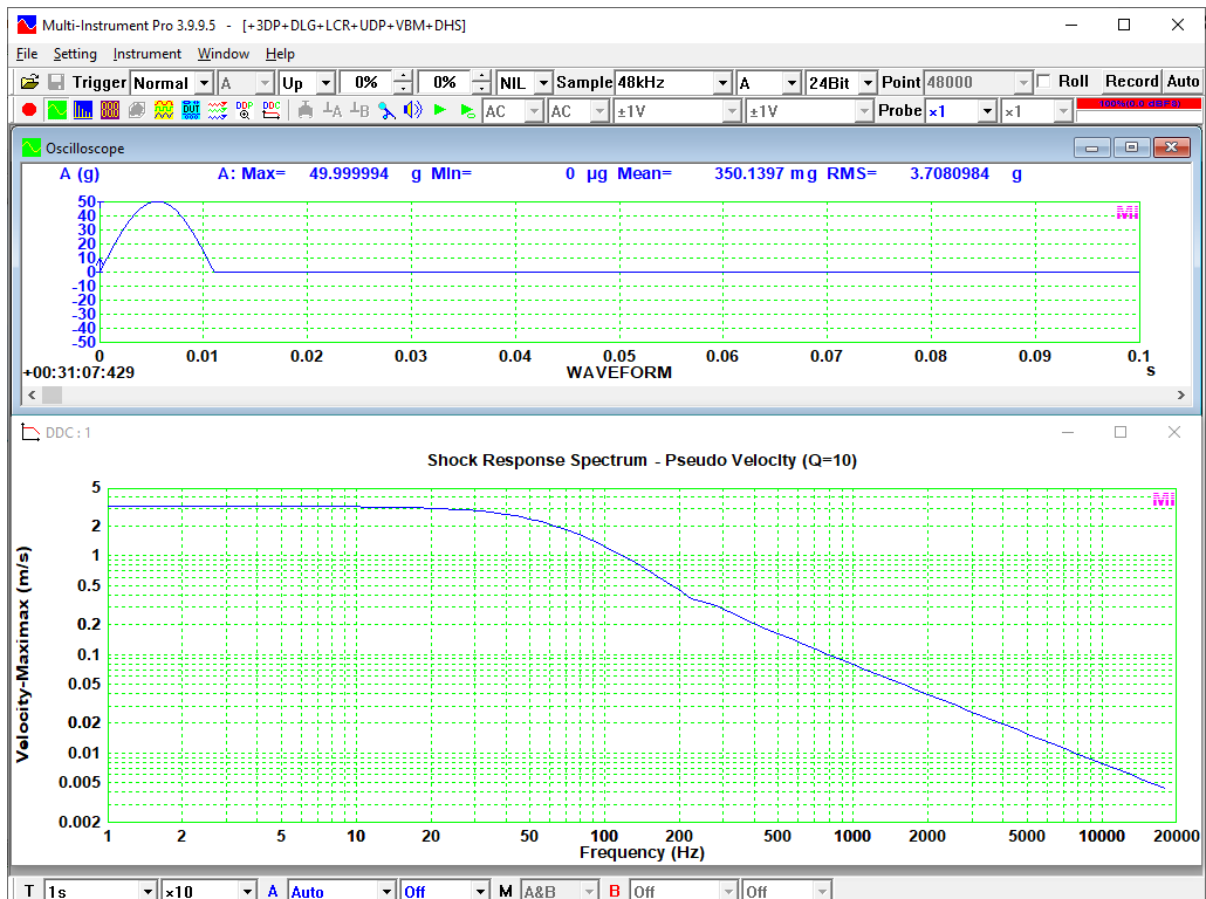


**Relative Displacement SRS of a Half-sine Pulse**

### 3.3.2.4 Pseudo Velocity Shock Response Spectrum

The following figures show the pseudo velocity SRS of a half-sine pulse, with a duration of 11 ms and a peak acceleration of 50g. The damping ratio used is 5% (i.e. Q=10).

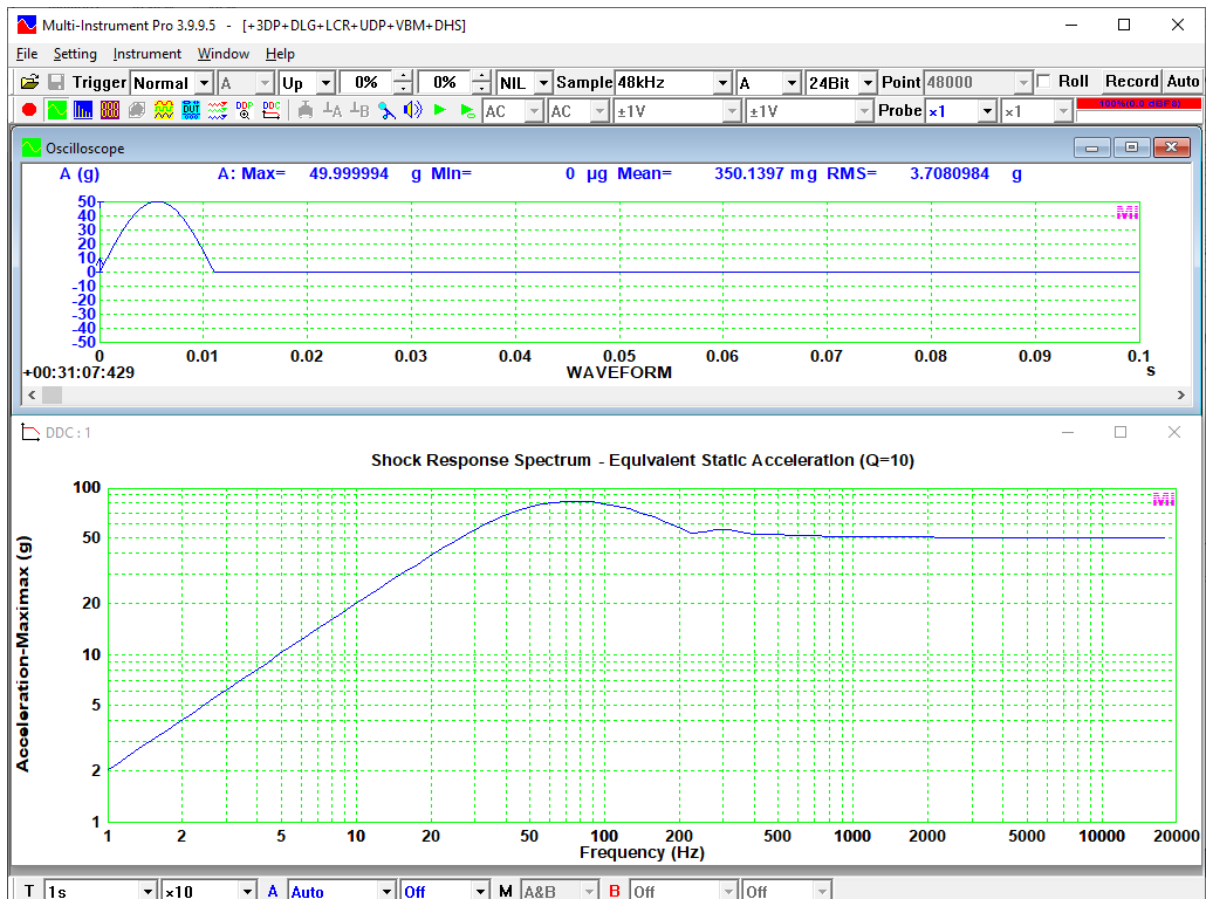




**Pseudo Velocity SRS of a Half-sine Pulse**

### 3.3.2.5 Equivalent Static Acceleration Shock Response Spectrum

The following figures show the equivalent static acceleration SRS of a half-sine pulse, with a duration of 11 ms and a peak acceleration of 50g. The damping ratio used is 5% (i.e.  $Q=10$ ).



**Equivalent Static Velocity SRS of a Half-sine Pulse**

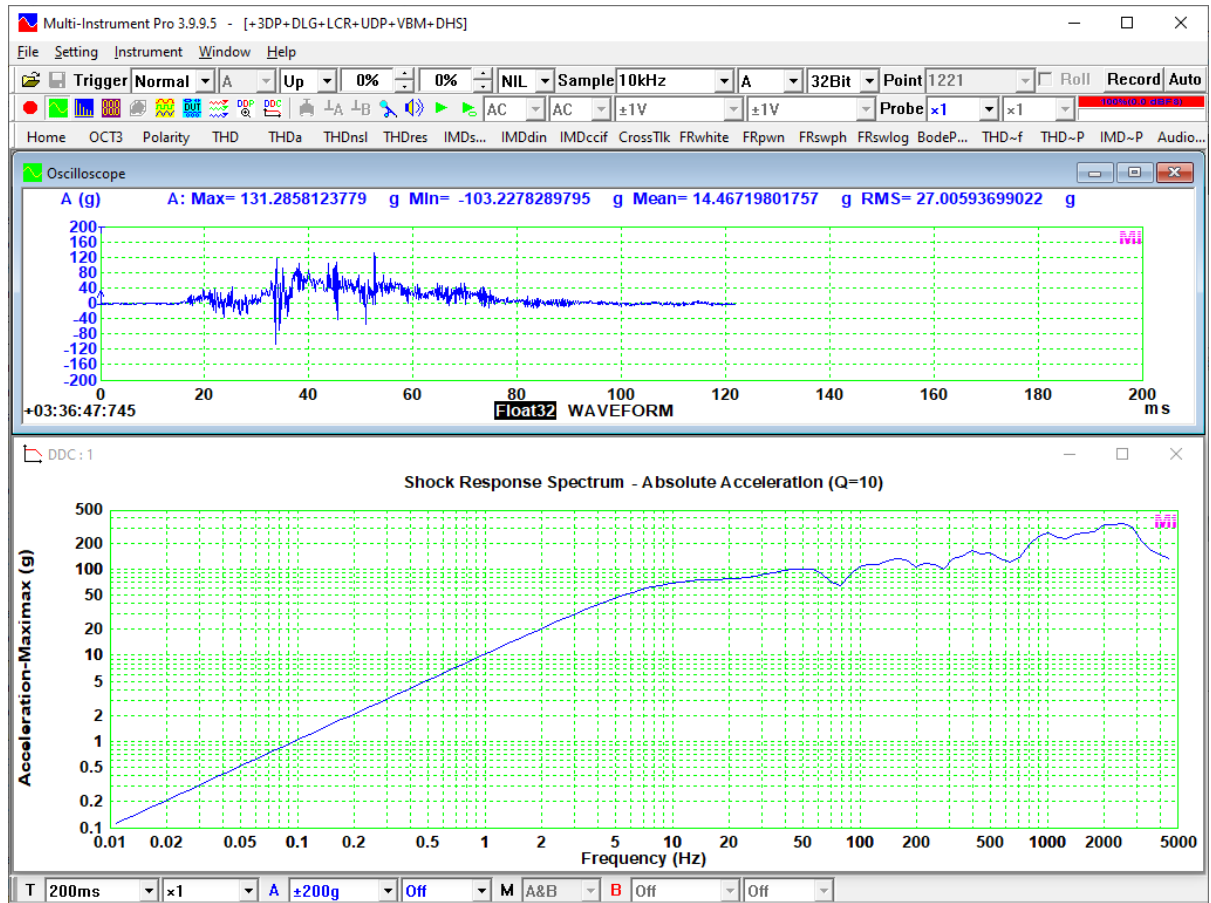
### 3.3.3 Car and Motorcycle Crash Test



**A Car and Motorcycle Crash Test**

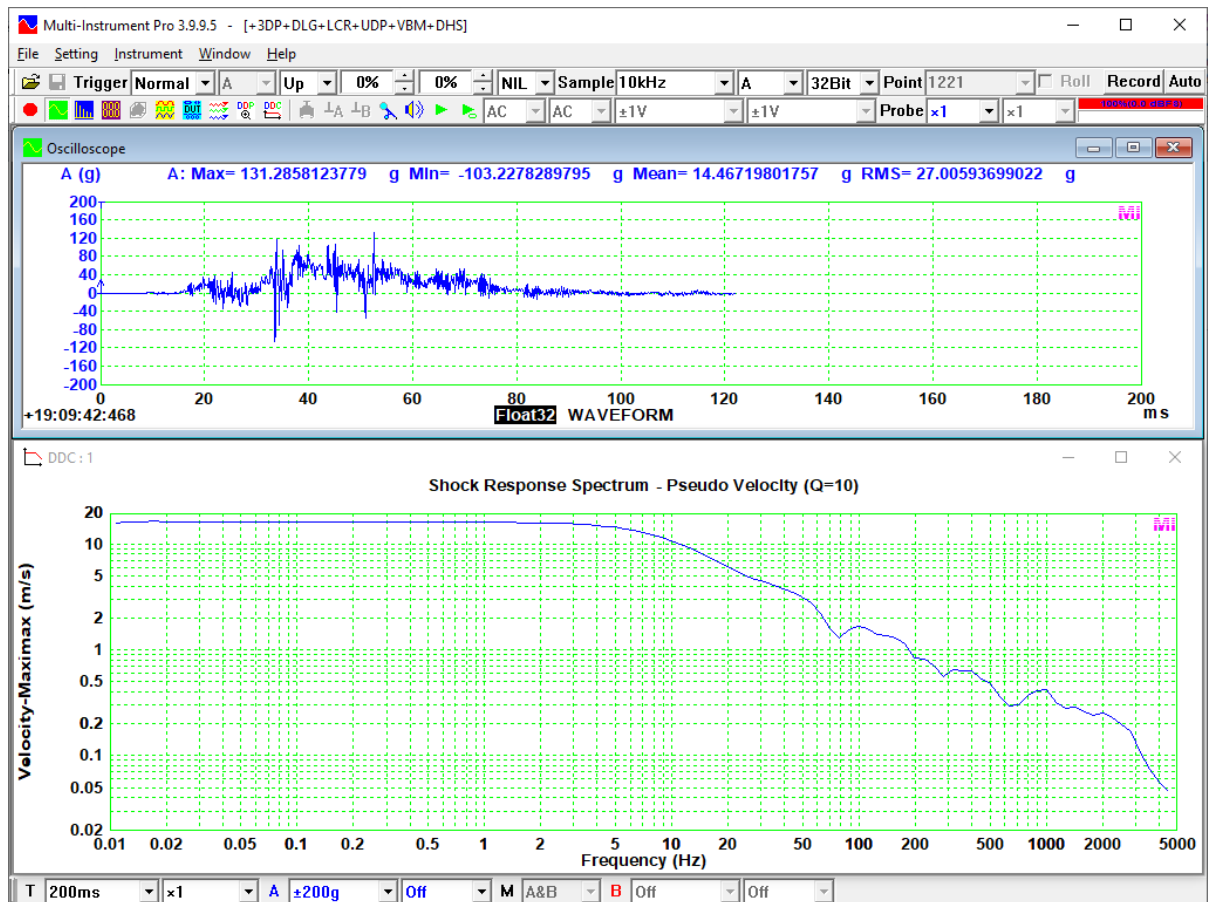
The acceleration data were recorded at the center of gravity of the motorcycle during a car and motorcycle crash test. The sampling rate of the acceleration data is 10kHz. The unit is g.

### 3.3.3.1 Absolute Acceleration Shock Response Spectrum



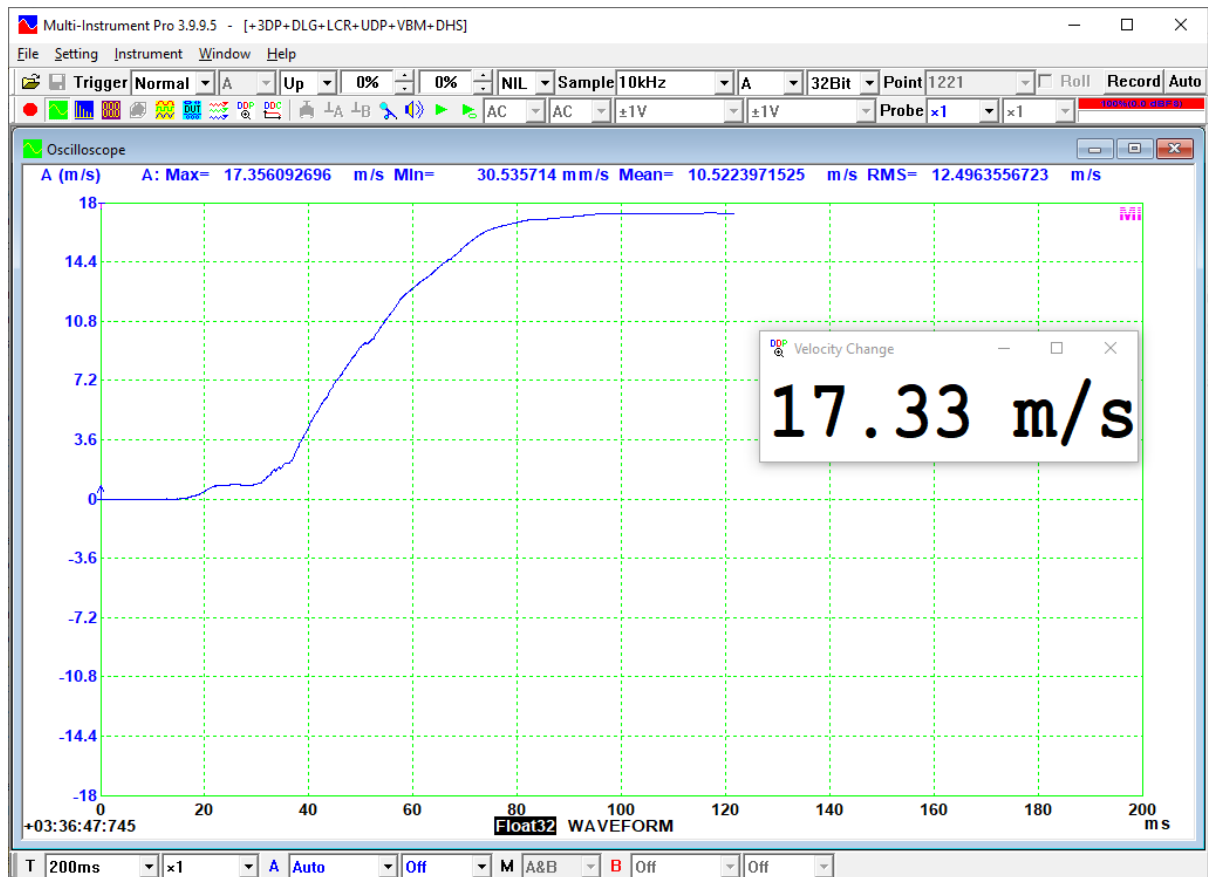
**Absolute Acceleration SRS of a Car and Motorcycle Crash Test**

### 3.3.3.2 Pseudo Velocity Shock Response Spectrum



**Pseudo Velocity SRS of a Car and Motorcycle Crash Test**

### 3.3.3.3 Velocity Change



**Velocity Change of a Car and Motorcycle Crash Test**

### 3.3.4 Barge Shock Test

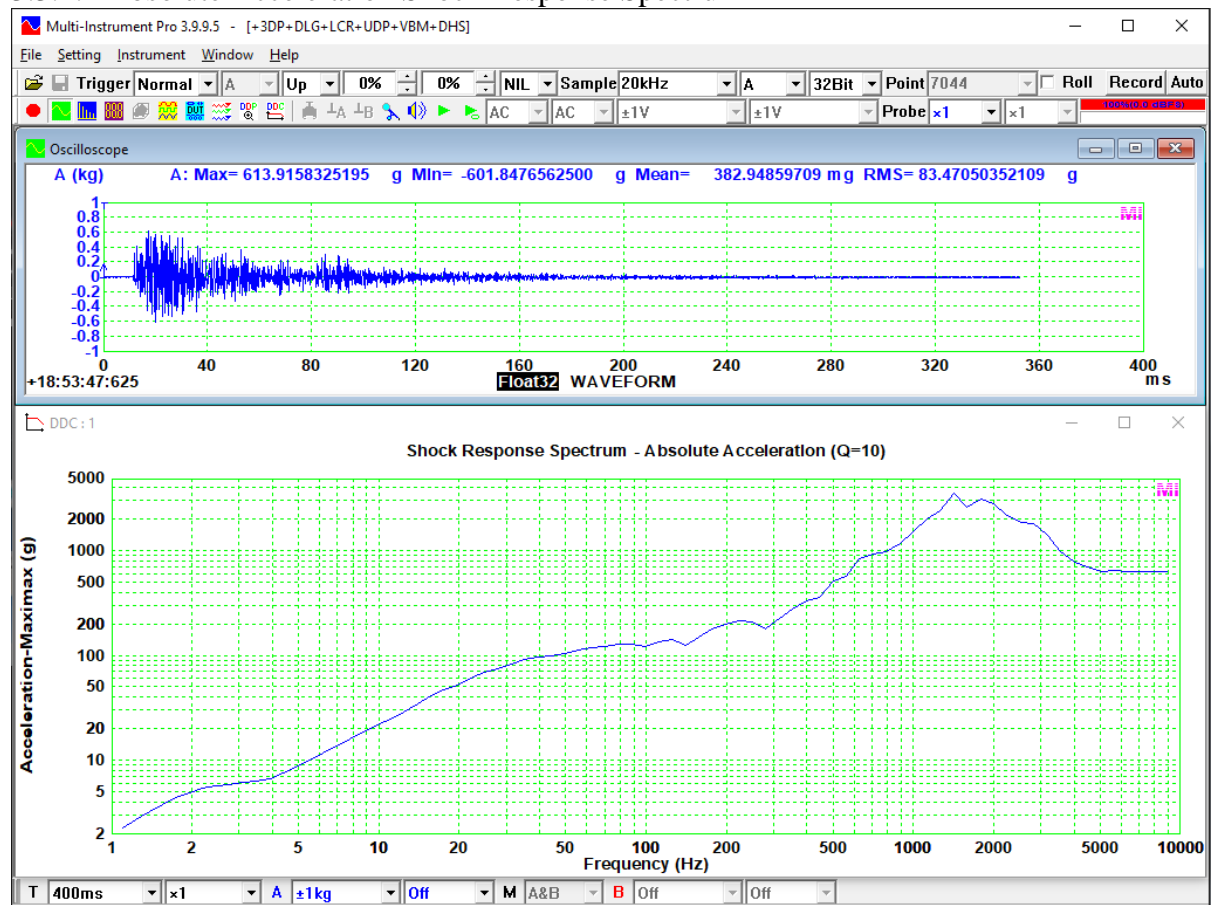


**A Barge Shock Test**

This acceleration signal was recorded during a MIL-S-901D barge shock test. The test was used to assess the quality of shipborne equipment under high-impact mechanical shocks,

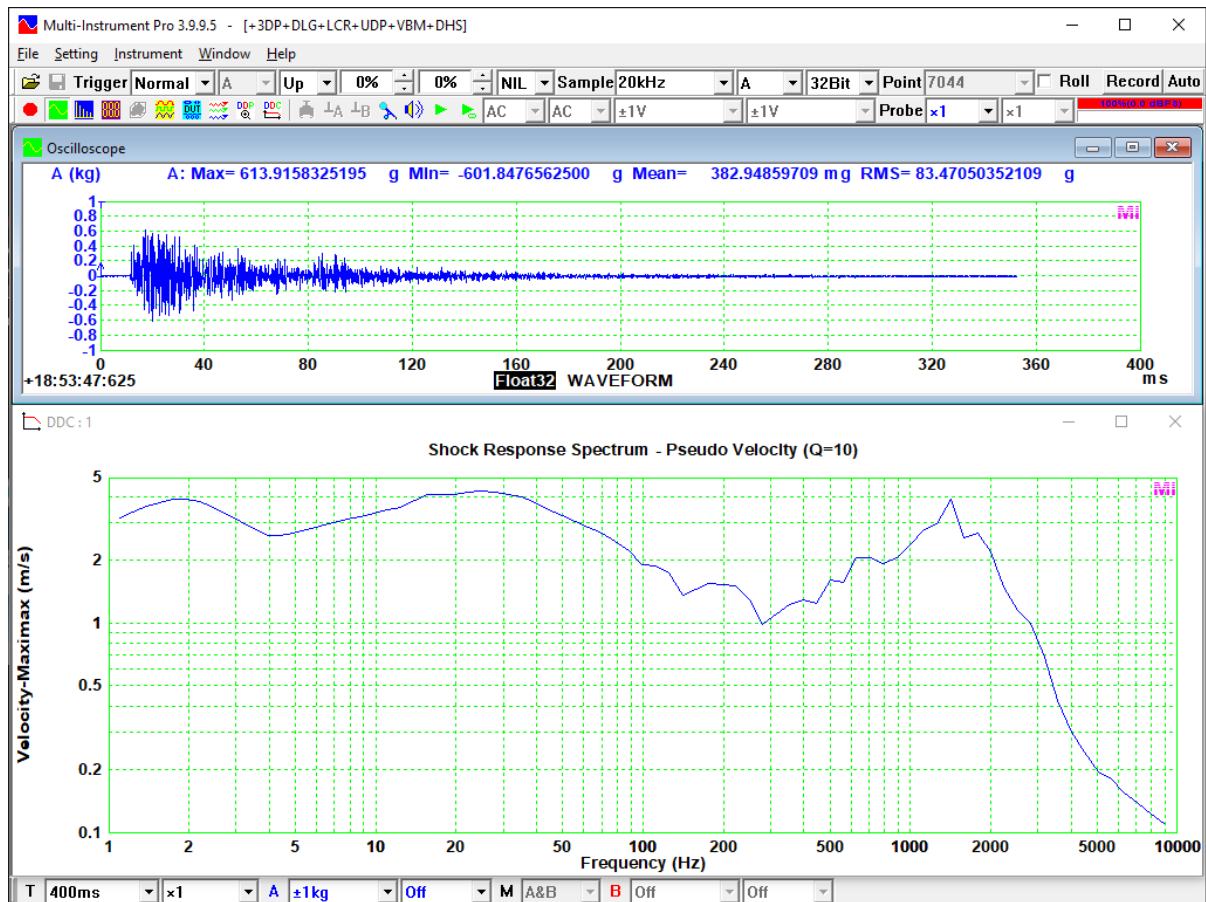
such as a torpedo explosion. The sampling rate of the acceleration data is 20kHz. The unit is g.

### 3.3.4.1 Absolute Acceleration Shock Response Spectrum



**Absolute Acceleration SRS of A Barge Shock Test**

### 3.3.4.2 Pseudo Velocity Shock Response Spectrum



**Pseudo Velocity SRS of A Barge Shock Test**

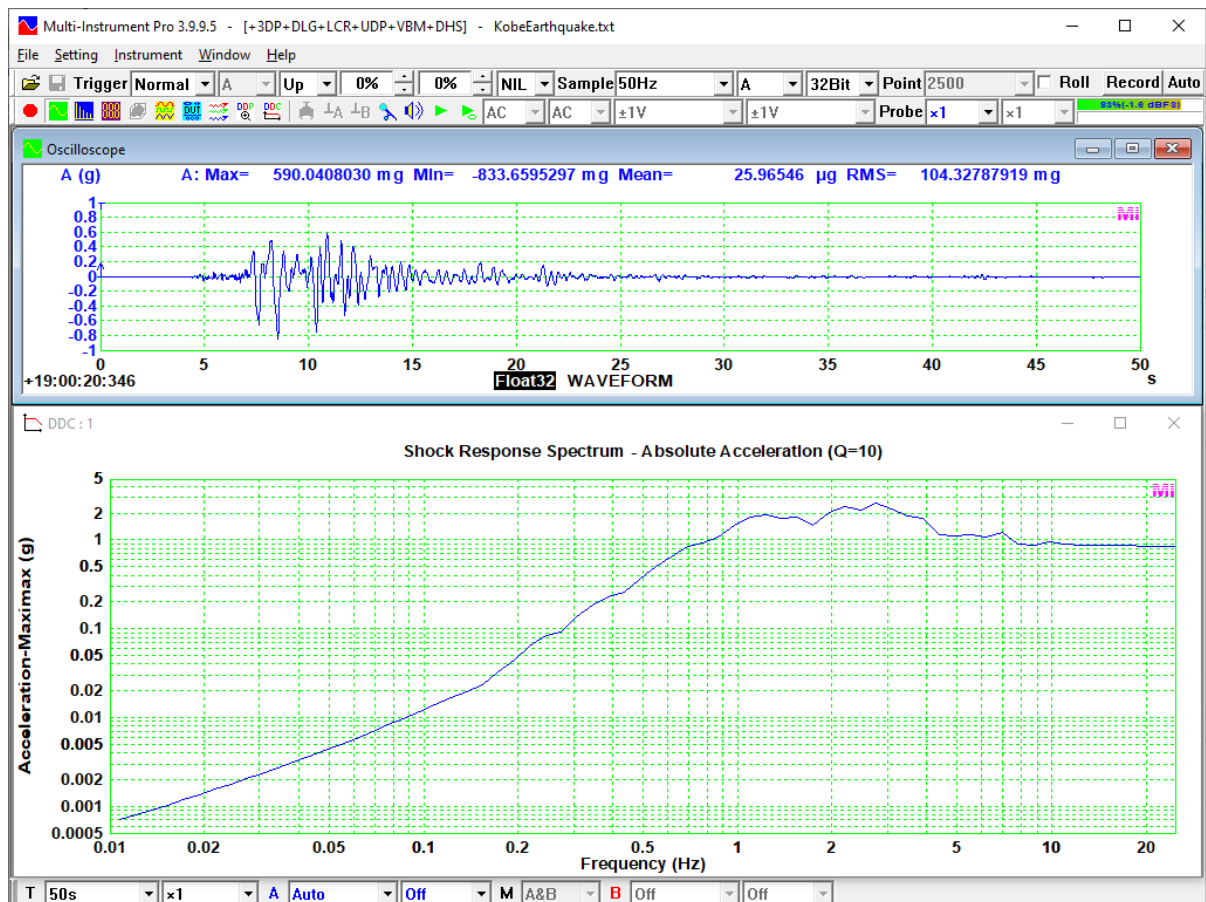
### 3.3.5 Kobe Earthquake Signal

This earthquake acceleration signal is the north-south component recorded at Kobe Japanese Meteorological Agency (JMA) station during the Hyogo-ken Nanbu (Kobe) earthquake of Jan. 17, 1995. The magnitude is 7.2. The sampling rate of the acceleration data is 50Hz. The unit is g.



**Kobe Earthquake 1995**

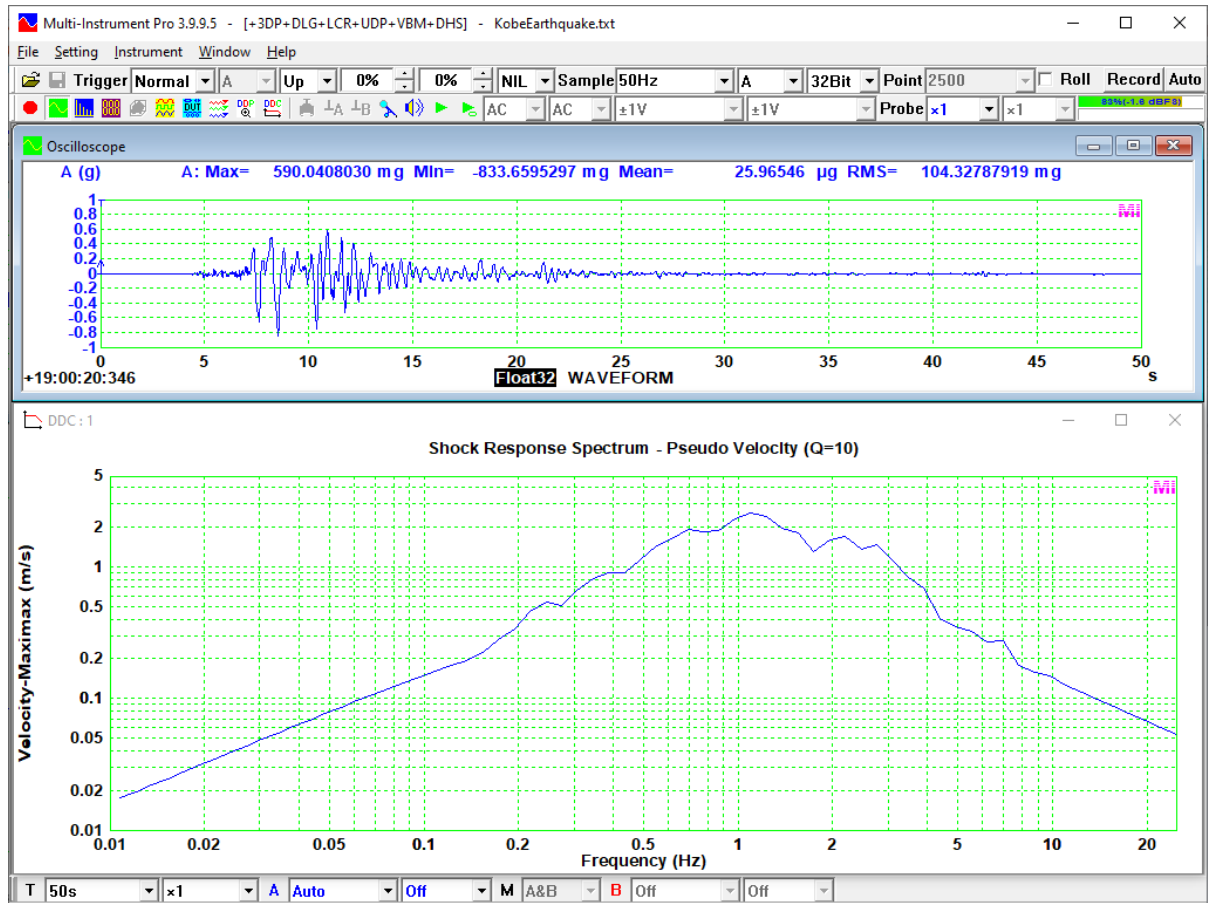
### 3.3.5.1 Absolute Acceleration Shock Response Spectrum



**Absolute Acceleration SRS of Kobe Earthquake**



### 3.3.5.2 Pseudo Velocity Shock Response Spectrum



**Pseudo Velocity SRS of Kobe Earthquake**